Front. Struct. Civ. Eng. 2014, 8(1): 57–68
DOI 10.1007/s11709-014-0235-0

RESEARCH ARTICLE

# Numerical simulations of morphological changes in barrier islands induced by storm surges and waves using a supercritical flow model

**Soumendra Nath KUIRY[a], Yan DING[b,*], Sam S Y WANG[b]**

[a] *Environmental & Water Resources Engineering Division, Department of Civil Engineering, Indian Institute of Technology Madras, Tamil Nadu 600036, India*

[b] *National Center for Computational Hydroscience and Engineering, The University of Mississippi, University, MS 38677, USA*

[*] *Corresponding author. E-mail: ding@ncche.olemiss.edu*



**ABSTRACT** In this paper, an advanced explicit finite volume flow model in two-dimensions is presented for simulating supercritical coastal flows and morphological changes in a tidal/coastal inlet and barrier islands due to storm surges and waves. This flow model is coupled with existing wave-action model and sediment transport model. The resulting integrated coastal process model is capable of simulating flows induced by extreme conditions such as waves, surge tides, river flood flows, etc., and morphological changes induced by rapid coastal currents and waves. This developed supercritical flow model is based on the solution of the conservative form of the nonlinear shallow water equations with the effects of the Coriolis force, uneven bathymetry, wind stress, and wave radiation stresses. The forward Euler scheme is used for the unsteady term; and the convective term is discretized using the Godunov-type shock-capturing scheme along with the HLL Riemann solver on non-uniform rectilinear grids. The accuracy of the developed model is investigated by solving an experimental dam-break test case. Barrier island breaching, overflow and overwash due to severe storm attack are simulated and the predicted morphological changes associated to the events are analyzed to investigate the applicability of the model in a coast where all the physical forces are present.

**KEYWORDS** coastal inlet, coastal process modeling, supercritical flow, sediment transport, barrier islands

## 1 Introduction

During extreme hydrological conditions induced by a tropical storm or a hurricane, high waves riding on the rising sea water, constantly pushing beaches and coastlines, may overflow, overwash, and breach coastal levees and barrier islands. Due to wave runup and inundation of flooding waters, strong currents together with storm surges may severely erode sand beach and barrier islands, create deep local scouring around coastal structures, and make drastic shoreline changes (e.g., Briaud et al. [1]). Hazardous coastal flood/inundation and morphological changes due to surges and high waves can further cause property damages and loss of lives (e.g., Fritz et al. [2]). Due to strong currents and rapid changes in bathymetry, coastal flow may become complex and supercritical when it overwashes top of levees or barrier islands, or it surges through a coastal/tidal inlet. For development of a resilient coastal community, better coastal hazard management and designs of coastal structures are needed to consider such extreme conditions in order to protect coastal zones from disastrous flooding/inundation and severe morphological changes. For instances, extreme tropical storm hydrological conditions and their impacts on morphological changes around coastal infrastructures were carefully studied for planning the Lousiana coastal protection and restoration (e.g., LACPR [3]) and the Mississippi Gulf coast defense (e.g., MsCIP [4]).

Coastal/tidal inlets along barrier islands are used to facilitate exchange of fresh and saline water, navigation and pathway for sediments, nutrients, water-borne materials etc. Such inlets and islands are often attacked by ocean

*Article history: Received May. 9, 2013; Accepted Oct. 21, 2013*

waves, tides, and storm surges, resulting in significant erosion, sediment movement, and bed changes of inlet channel and instability of the shoreline at the adjacent coasts. The model such as DUROSTA [5] focuses on sand supplies to the swash and surf zones by the backwash motion and by the undertow. Overton and Fisher [6], Nishi and Kraus [7] studied the supply of sand by the dune based on the concept of wave impact. The variety of models range from empirical formulations (e.g., Stockdon et al. [8]) through analytical approaches [9,10] to numerical models in one-dimension (e.g., Roelvink [11]) and in two-dimension (e.g., Refs. [12,13]). Roelvink et al. [14] used the combination of shallow water equations and standard suspended transport model to study breaching of sand barrier. Militello and Kraus [15] and Ding and Wang [16] reported that morphodynamic response of an inlet to tides and storm waves can lead to ebb and flood shoals formation, navigation channel refilling, migration of the channel thalweg, skewing of ebb shoals, development of tip shoals, beach erosion, and formation of scour holes inside the inlet and adjacent to the jetty tips. The hydrodynamics and morphodynamics associated to these problems may be investigated effectively and efficiently using process based numerical models.

In recent years numerical flow models have been increasingly popular and applied to simulate coastal flows and morphological changes due to storm surge, wave or tsunami (e.g., Refs. [1,17–20]). Modeling the effects of these extreme events is important for design of coastal structures, sediment management, shoreline protection, maintenance of navigation channel, etc. The numerical models can be used in a cost effective way comparing to physical model study in order to refine and optimize designs of coastal structures.

In this study, a process-based supercritical coastal flow model is developed to simulate overflow and overwash due to rapid currents driven by storm surges and waves through a coastal inlet, as well as morphological changes in the inlet and barrier islands. This flow model is integrated with two existing submodels: (1) wave-action model and (2) sediment transport model. The wave-action submodel (i.e., CMS-Wave, Lin et al. [21]) and sediment transport submodel of the SMS (Surfacewater Modeling System) (Zundel [22]) are systematically used with the developed hydrodynamic model to simulate all the physical processes. Based on the Godunov-type scheme along with the HLL Riemann solver (Harten et al. [23]), the supercritical flow model is developed to enable the integrated coastal process model to simulate overflow and overwash flow induced by storm surges and waves. The supercritical model solves the conservative form of the nonlinear shallow water equations (SWEs) in which the effects of the Coriolis force, surface wind stress, bottom roughness, uneven bathymetry and short wave-averaged radiation stresses are included. The Godunov-type method represents physically correct propagation of information throughout the flow field by solving a set of local Riemann problems. The radiation stresses which are obtained by simulating the wave field using the wave-action model are added as source term in the momentum equations to represent the long shore current. The simulated flow field is used by the sediment transport submodel, and the bathymetry is updated at a given time interval. As a result, the developed coastal process model calculates waves, currents, sediment transport, and morphological changes sequentially under the combined conditions of surge tides and storm waves.

The supercritical flow model is validated carefully by simulating dam-break wave propagation over a triangular obstacle; and then the integrated model is applied to simulate hydrodynamic and morphodynamic responses to a hypothetical surge tide and wave in a coast with barrier islands and inlet. Barrier island breaching, overflow and overwash due to severe storm attack are also simulated and the morphodynamic changes associated to the events are analyzed to investigate the applicability of the model in a coast where all the physical forces are present.

## 2 Model description

The hydrodynamic model is integrated with the wave and sediment transport models readily available in SMS [18] and all the three models can be operated sequentially. Thus the coastal process model uses several differential equations and they are solved in a decoupled way. The wave model computes wave parameters (i.e., wave heights, periods, and directions) and radiation stresses and they are included as source terms in the hydrodynamic model in order to accurately represent longshore current of the flow field. Once the flow field is computed, the cross-shore and longshore sediment transport fluxes are calculated using the sediment transport model based on the Lund-CIRP total load formulation [24]. The details of the governing equations and solution methods of the models are briefly described below.

### 2.1 Wave model

The CMS-Wave [21] takes into account the effect of an ambient horizontal current or wave behavior and solves the wave-action balance equation as

$$\frac{\partial(v_x N)}{\partial x}+\frac{\partial(v_y N)}{\partial y}+\frac{\partial(v_\theta N)}{\partial \theta} =\frac{\kappa}{2\sigma}\left[(CC_{\mathrm{g}}\cos^2\theta N_y)_y-\frac{CC_{\mathrm{g}}}{2}\cos^2\theta N_{yy}\right]-\varepsilon_{\mathrm{b}}N-R, \quad (1)$$

where $N=E(\sigma,\theta)/\sigma$ is the wave-action density to be solved and is a function of frequency $\sigma$ and direction $\theta$. The spectral wave density $E(\sigma,\theta)$ represents the wave energy per unit water surface area per frequency interval. In

Eq. (1), $C$,$C_g$ = wave celerity and group velocity, respectively; $x$,$y$ = horizontal coordinates in two directions; $v_x$,$v_y$ and $v_\theta$ = characteristic velocity components with respect to $x$,$y$ and $\theta$; $N_y$,$N_{yy}$ = first and second derivatives with respect to $y$, respectively; $\kappa$ = empirical constant representing the intensity of diffraction effect; $\varepsilon_b$ = parameterization of wave breaking energy dissipation and $R$ = source terms (e. g., wind forcing, bottom friction loss, nonlinear wave-wave interaction term). The term $\kappa$ needs to be calibrated and optimized for structures. The velocity components in Eq. (1) are given by

$$v_x = C_g \cos\theta + u, \tag{2}$$

$$v_y = C_g \sin\theta + v, \tag{3}$$

$$v_\theta = \frac{C_g}{C}\left(\sin\theta\frac{\partial C}{\partial x} - \cos\theta\frac{\partial C}{\partial y}\right), \tag{4}$$

where $u$,$v$ = depth-averaged horizontal current velocity components along $x$ and $y$ directions.

## 2.2 Flow model

A depth and shortwave-averaged form of the SWEs are used for simulating currents induced by tides and waves [25]. The governing equations in conservative form can be written as follows:

$$\frac{\partial \mathbf{U}}{\partial t} + \frac{\partial \mathbf{E}(\mathbf{U})}{\partial x} + \frac{\partial \mathbf{G}(\mathbf{U})}{\partial y} = \mathbf{S}(x,y,\mathrm{U}), \tag{5}$$

in which,

$$\mathbf{U} = \begin{bmatrix} H \\ H_u \\ H_v \end{bmatrix};$$

$$\mathbf{E} = \begin{bmatrix} Hu \\ Hu^2 + \frac{1}{2}gH^2 \\ Huv \end{bmatrix};$$

$$\mathbf{G} = \begin{bmatrix} Hv \\ Huv \\ Hv^2 + \frac{1}{2}gH^2 \end{bmatrix},$$

$$\mathbf{S} = \begin{bmatrix} 0 \\ gH\frac{\partial h}{\partial x} + f(Hv) + \frac{\partial}{\partial x}\left(D_x\frac{\partial(Hu)}{\partial x}\right) + \frac{\partial}{\partial y}\left(D_y\frac{\partial(Hu)}{\partial y}\right) - \tau_{bx} + \tau_{sx} + \tau_{wx} \\ gH\frac{\partial h}{\partial y} - f(Hu) + \frac{\partial}{\partial x}\left(D_x\frac{\partial(Hv)}{\partial x}\right) + \frac{\partial}{\partial y}\left(D_y\frac{\partial(Hv)}{\partial y}\right) - \tau_{by} + \tau_{sy} + \tau_{wy} \end{bmatrix},$$

where $\mathbf{U}$ = vector of conserved variables; $\mathbf{E}$ and $\boldsymbol{G}$ = convective fluxes in the $x$ and $y$ directions, respectively; and $\mathbf{S}$ = source term. In addition, $h$ = still water depth from a datum (see Fig. 1); $\eta$ = deviation of the water surface from the still water level; $H = (h + \eta)$ = total water depth; $u$ and $v$ = depth-averaged current velocities parallel to the $x$ and $y$ directions; $g$ = acceleration due to gravity; $f$ = Coriolis force with $f = 2\omega\sin\varphi$, in which $\omega$ = angular frequency of earth rotation, and $\varphi$ = latitude. The other parameters in the $x$ and $y$ directions are: $S_{0x}$ and $S_{0y}$ = bed slopes; $D_x$ and $D_y$ = diffusion coefficients; $\tau_{bx}$ and $\tau_{by}$ = bed shear stresses; $\tau_{sx}$ and $\tau_{sy}$ = wave stresses; $\tau_{wx}$ and $\tau_{wy}$ = surface wind stresses, respectively.

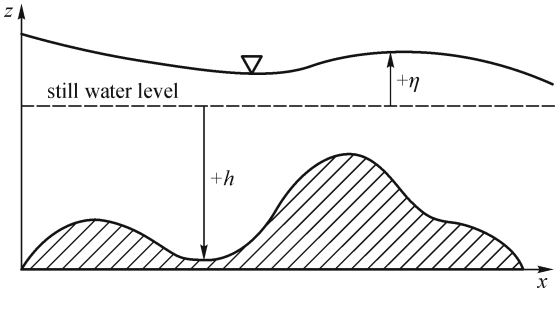


**Fig. 1** Definition sketch for bed topography, water depth and water surface elevation

## 2.3 Sediment transport and morphodynamic change model

The sediment transport model is based on the calculations of sediment transport rates and resultant changes in water depth (bottom elevation) through gradients in transport rates as proposed in Lund-CIRP formulations [24]. Bed level changes are obtained from the sediment continuity equation:

$$\frac{\partial h}{\partial t} = \frac{1}{1-p}\left(\frac{\partial q_{bx}}{\partial x} + \frac{\partial q_{by}}{\partial x} + P - D\right), \tag{6}$$

where $q_{bx}$,$q_{by}$ = bed load transport rate in the $x$- and $y$-directions, respectively and $p$ = porosity of sediment. The term $\partial q_{bx}/\partial x + \partial q_{by}/\partial y$ represents the bed load component and the term $P - D$ corresponds to the suspended load component. While evaluating the bed changes by Eq. (6), time-averaged transport rates are used ($\overline{q}_{bx}$,$\overline{q}_{by}$). In this approach, instantaneous transport rates are computed at a

time interval of $\Delta t_{sed}$ and time-averaged transport rates and morphological changes are calculated at a time interval of $\Delta t_{morph}$. Also, the bed load components in Eq. (6) are corrected for the slope effect as

$$\overline{q}_{bx}^{'} = \overline{q}_{bx} - D_s|\overline{q}_b|_x\frac{\partial h}{\partial x}, \tag{7}$$

$$\overline{q}_{by}^{'} = \overline{q}_{by} - D_s|\overline{q}_b|_y\frac{\partial h}{\partial y}, \tag{8}$$

where $\overline{q}_b = \sqrt{\overline{q}_{bx}^2 + \overline{q}_{by}^2}$. Finally, Eq. (9) is solved to compute depth changes at the time interval $\Delta t_{morph}$:

$$\frac{\partial h}{\partial t} = \frac{1}{1-p}\left(\frac{\partial \overline{q^{'}}_{bx}}{\partial x} + \frac{\partial \overline{q^{'}}_{by}}{\partial x} + \overline{P} - \overline{D}\right). \tag{9}$$

Camenen and Larson [24] proposed a general transport formula for bed load under combined effect of wave and current as

$$\frac{q_{bw}}{\sqrt{(s-1)gd_{50}^3}} = a_w\sqrt{\theta_{net}}\theta_{cw,m}\exp\left(-b\frac{\theta_{cr}}{\theta_{cw}}\right), \tag{10}$$

$$\frac{q_{bn}}{\sqrt{(s-1)gd_{50}^3}} = a_n\sqrt{\theta_{cn}}\theta_{cw,m}\exp\left(-b\frac{\theta_{cr}}{\theta_{cw}}\right), \tag{11}$$

where subscripts w and n represent wave direction and direction normal to the wave, respectively; $d_{50}$ = median grain diameter; $\theta_{cr}$ = critical shields parameter; $s$ = specific gravity; $a_w$,$a_n$ and $b$ = empirical constants and $\theta_{cwm}$,$\theta_{cw}$ = mean and maximum shields parameter respectively. The quantities $\theta_{net}$ and $\theta_{cn}$ represent the net contribution of the shear stress to the transporting velocity during a wave cycle in the direction parallel and normal to the waves, respectively.

The suspended load $q_s$ is computed assuming an exponential concentration profile and a constant velocity over the water column and can be expressed as

$$q_s = uc_R\frac{\varepsilon}{w_s}\left(1 - e^{-\frac{w_s h}{\varepsilon}}\right), \tag{12}$$

where $w_s$ = sediment settling velocity, $c_R$ = reference concentration and $\varepsilon$ = sediment diffusivity (or turbulent mixing coefficient). The transport $q_s$ is considered to be taken place in the direction of current because the waves are assumed to produce a zero net drift and do not contribute to the suspended sediment transport.

## 3 Solution methods

To simulate coastal hydro and morphological processes, the governing partial differential equations for the three submodels, i.e., the energy balance equation (Eq. (1)), the depth- and wave-averaged continuity and momentum equation (Eq. (5)) and the seabed level evolution equation (Eq. (9)) are solved numerically. The integrated model is developed on a non-uniform rectangular Cartesian coordinate system. Though the wave and morphodynamic change models are used directly from the SMS in the present study, a brief description of the solution schemes of the submodels are presented in the following sections.

### 3.1 Wave model

The energy balance Eq. (1) is solved by means of parabolic approximation, in which the waves are assumed to have a principal propagation direction from offshore to onshore. Therefore, the computations are carried out line by line from offshore to onshore. The first term of Eq. (1) is discretized by forward difference scheme, second and third terms are discretized by QUICK scheme as proposed in Leonard [26], the diffraction term is discretized by central difference scheme and the source term is obtained by solving algebraic equations. Consequently, Eq. (1) is expressed in a finite difference form and is solved explicitly. The implementation of the numerical scheme is described in detail in Mase et al. [27,28].

### 3.2 Hydrodynamic model

A cell centered finite volume method is used to discretize Eq. (5) over a non-uniform rectangular control volume in a Cartesian grid with the assumption that the dependent variables are represented as piecewise constants. It is useful to rewrite Eq. (5) as

$$\frac{\partial \mathbf{U}}{\partial t} + \nabla\cdot\mathrm{F}(\mathbf{U}) = \mathbf{S}(x,y,\mathbf{U}), \tag{13}$$

in which $\mathrm{F} = (\mathrm{E},\mathrm{G})$ is the flux tensor, in order to introduce integral form of the equations over a fixed control volume $\Omega$:

$$\int_\Omega \frac{\partial \mathbf{U}}{\partial t}\mathrm{d}\Omega + \int_\Omega(\nabla\cdot\mathbf{F})\mathrm{d}\Omega = \int_\Omega \mathbf{S}\mathrm{d}\Omega. \tag{14}$$

In the 2D approach, a discrete form of Eq. (14) is applied to each cell $\Omega$ with dimension $(\Delta x,\Delta y)$ so that the volume integrals represent integrals over the area of the cell and the surface integrals represent the total flux through the cell boundary $\Gamma$. Assuming $\mathbf{U}$ as the average value of the conservative variables over the volume $\Omega$ at a given time, from Eq. (14) and applying Gauss divergence theorem to the second integral, the conservation equation can be written as

$$A\frac{\partial \mathbf{U}}{\partial t} + \oint_\Gamma(\mathbf{F}\cdot n)\mathrm{d}\Gamma = A\mathbf{S}, \tag{15}$$

where $A$ is the cell area and $\boldsymbol{n}$ is the unitary outward

normal.

A two-dimensional discrete finite volume formulation of the system of Eq. (15) with explicit scheme, which applies forward Euler discretization to time derivative, on a non-uniform rectilinear grid ($\Delta x$,$\Delta y$), leads to the inherently conservative method:

$$\mathbf{U}_{i,j}^{n+1} = \mathbf{U}_{i,j}^{n} - \frac{\Delta t}{\Delta x}\left(\mathbf{E}_{i+1/2,j}^{*} - \mathbf{E}_{i-1/2,j}^{*}\right) - \frac{\Delta t}{\Delta y}\left(\mathbf{G}_{i,j+1/2}^{*} - \mathbf{G}_{i,j-1/2}^{*}\right) + \Delta t \mathbf{S}_{i,j}, \qquad (16)$$

in which $\mathbf{F}_{i\pm1/2}^{*} = (\mathbf{E}_{i\pm1/2}^{*}, \mathbf{G}_{i\pm1/2}^{*})$ = numerical convective flux functions through the cell interfaces $\Gamma_{i\pm1/2,j}$ and $\Gamma_{i,j\pm1/2}$ (Fig. 2) respectively; $\Delta t$ = time step size and $\mathbf{S}_{i,j}$ = a discretization of the source term. In this study, HLL Riemann solver [23] is chosen for convective flux ($\mathbf{F}^{*}$) computation.

### 3.3 Sediment transport and morphodynamic change model

In the present study the Lund-CIRP model available in SMS is used to compute bed evolution. In this submodel, the sediment transport properties and transport rates are calculated at the cell centers. After transport rates are calculated by the Lund-CIRP formulae for all the cells in the domain, they are mapped back to the cell faces such that $x$ directed rate is located on the left face center and the $y$ directed rate is located on the bottom face center. These instantaneous transport rates are calculated at the sediment transport time step $\Delta t_{\text{sed}}$ and instantaneous rates averaged over the morphologic change time step are evaluated at the time step $\Delta t_{\text{morph}}$. The Eq. (9) is then solved for every cell by means of forward Euler scheme to compute the bed changes over the time period $\Delta t_{\text{morph}}$. The implementation of the model is explained in Buttolph et al. [18].

## 4 Model application

Since the wave and sediment transport models are verified and validated before [25], accuracy of the hydrodynamic model is investigated here and presented below. Then the coupled model is applied to a severe storm surge attacking a hypothetical coast with an inlet.

### 4.1 Flow over a triangular obstacle

This test is carried out to examine the ability and accuracy of the hydrodynamic model to simulate flows over a dry and irregular bathymetry. The experiment was conducted under the supervision of J. M. Hiver at the Laboratoire de Recherches Hydrauliques at Châtelet together with the University of Bruxelles (Belgium) [29]. The physical experiment includes complex hydraulic properties like a dam break flow, transitions between wet and dry bed, hydraulic jump and flows over an obstacle. The channel geometry is illustrated in Fig. 3. The experiment consists of a reservoir with water up to 0.75 m contained by a dam at $x = 15.5$ m and a dry bed downstream within a rectangular channel of length 22.5 m. A symmetric triangular obstacle (6 m long, 0.4 m high) is situated with its peak located at 14 m downstream the dam. A number of gauge points located on the bed of the channel at different distances from the dam are also shown in Fig. 3 and are at 4 m (G4), 10 m (G10), 11 m (G11), 13 m (G13), and at 20 m (G20). The gauge point G13 is located at the vertex of the obstacle and therefore is a critical point. At these gauge points water depth evolutions are measured. The fixed boundaries are walls except the free outlet and the Manning's roughness coefficient is taken as 0.0125 $m^{-1/3}s$, a value which has been supplied by the experimentalists [29]. In the computation, 0.1 m square size grids and $\Delta t = 0.01$ s are used. The water depth variations with respect to time at

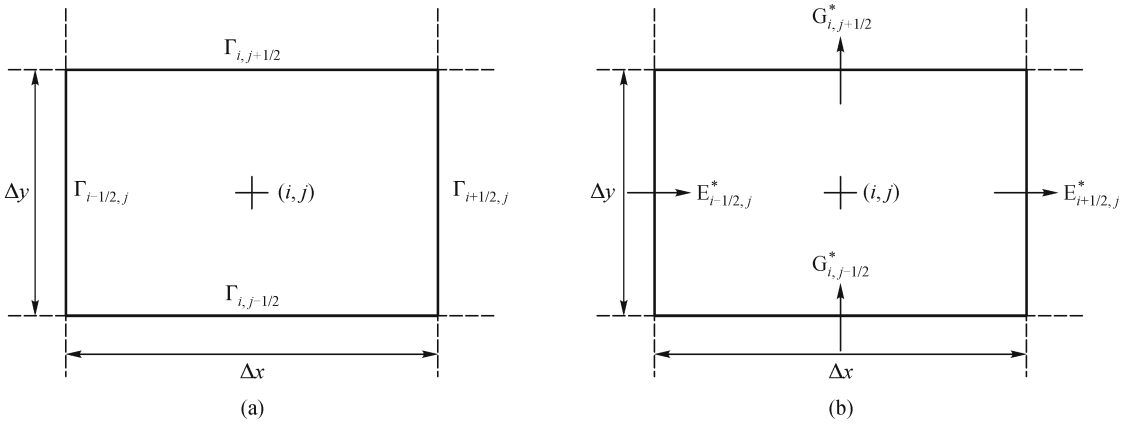


**Fig. 2** Discretization of a finite volume cell. (a) Interfaces; (b) numerical fluxes

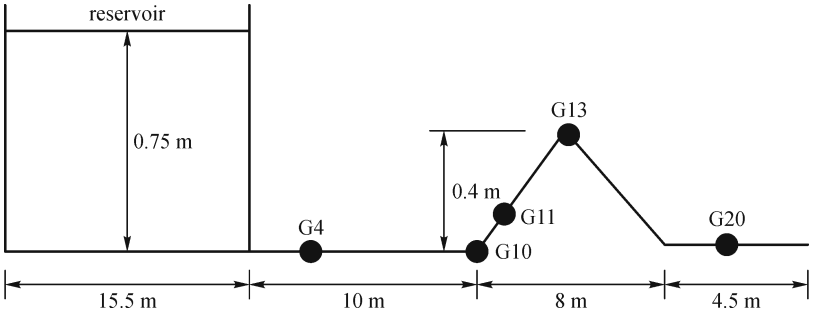


**Fig. 3** Geometry and gauge locations for the experimental and model set up

the gauge points are shown in Fig. 4. It can be seen that the water depth evolution and the prediction of arrival time of the wave to the corresponding gauge points are quite comparable with the experimental observations. The prediction of the transitions from wet to dry at the gauge point G13 is also well predicted. The maximum deviation is observed at station G20. However, the water depth at this point is very small and similar accuracy was reported by Brufau et al. [29].Thus it can be concluded that the present model accurately simulates the flow characteristics observed in the complex laboratory experiment.

### 4.2 Short-term morphodynamic simulation driven by storm surges and waves through a tidal inlet channel in a coast

During severe storm or hurricane, the barrier islands along a coast get seriously affected. The barrier islands may be overwashed and/or breached. Inlet channel may be developed through the breached area. The flood water passes through inlets and inundates the bay area. At the same time morphology of the coast also changes drastically. This may result in undermining the foundation of coastal structures, ebb and flood shoal formation. Sometimes existing navigation channel is refilled by migrated sediments. The study of hydraulics of such flow field and morphological changes are important for engineering design of inlet structures. The present model is applied to such an idealized coast with an inlet of 30 m wide. The coast is designed in such a way that it represents the basic geometry, inlet entrance configuration, offshore slope, wave and storm forcings at a medium size inlet. Figure 5 shows the flow domain with bathymetry varying from 30 m at offshore to dry bay. The inlet channel section is enlarged and is shown separately in the same Fig. 5.

The wave-current-morphodynamic processes in the coast are investigated when a severe storm surge attacks the coast. A rectangular grid is generated for the flow domain with the help of SMS grid generator with resolution 25 m in the channel and 50 m in the offshore. The three processes are simulated sequentially by the steering option of the SMS package. An irregular spectral wave with significant wave height $H_s = 3.5$m, a peak period $T_p = 9$ s, and mean incident angle $= 30^\circ$ (JONSWAP spectrum $\gamma = 3.3$) is imposed at the offshore boundary. Superimposed into a $M_2$ tide with amplitude of 0.5 m above the mean sea level, a storm surge shown in Fig. 6 with a peak of 10.0 m is also imposed at the offshore boundary. The other ocean boundaries are specified as free flow boundaries. The radiation stress gradients calculated from the specified wave is updated at an interval of 3 h. The uniform median grain size ($d_{50}$) in the coast is specified as 0.2 mm. The Lund-CIRP formulations as presented before are used to compute the total sediment transport rate and the bed evolution is calculated using Eq. (9).

In Figs. 7 and 8, the results are reported at two time intervals at 19 and 27 h, respectively. At 19 h, flood tide passes through the inlet, at 27 h ebb tide leaves the bay back into the sea. Both the flood and ebb tides induce strong velocities. Figure 7(a) shows the morphological changes and (b) velocity vectors with stream traces around the inlet during flood tide. Figure 8(a) shows the bed elevation changes and (b) velocity vectors with stream traces during the ebb tide at 27 h. The strong velocities cause significant erosion and develop scour hole at the entrance of the inlet and deposition at the bay side. Thus a flood shoal can be created in the bay which is frequently observed in a real coastal inlet. At 27 h, during the ebb tide, flow passes from the bay to the offshore direction. At this instant, bed erosion takes place at the entrance of ebb tide in the bay side and deposition takes place along the inlet channel. Thus the scour hole created during the flood tide is refilled and ebb shoal is formed at the offshore side (see the offshore in Fig. 7(a)). The computed bed profiles at different times along a transect A-A passing through the centerline of the inlet (Fig. 5) is plotted in Fig. 9. It is clearly shown that the severe erosion takes place at the entrance of the inlet and a scour hole is formed; the flood and the ebb shoals are developed in the channel and at the entrance of the inlet. Though the results shown in this

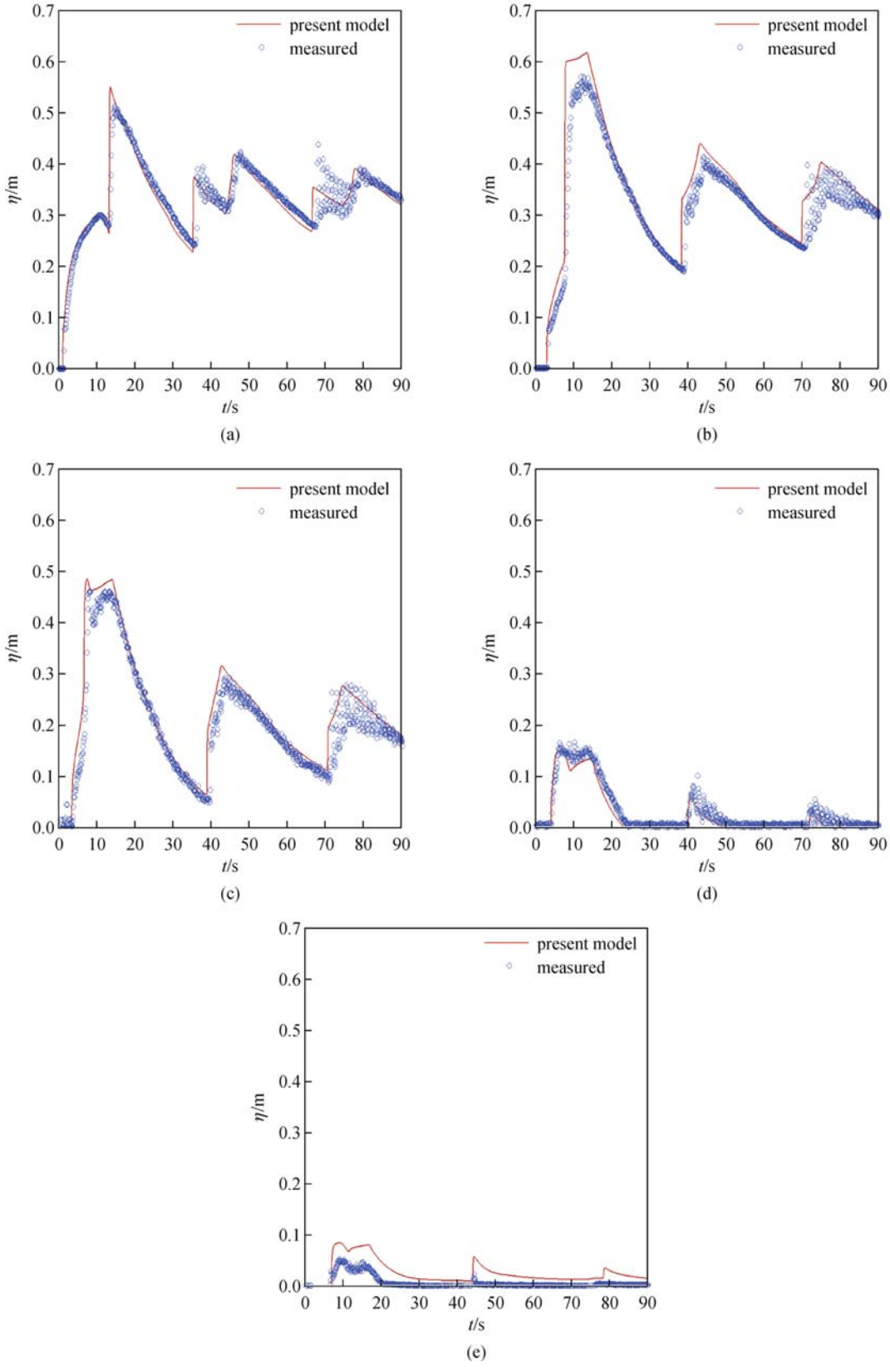


**Fig. 4** Computed and measured water depth variations at stations. (a) G4; (b) G10; (c) G11; (d) G13; (e) G20

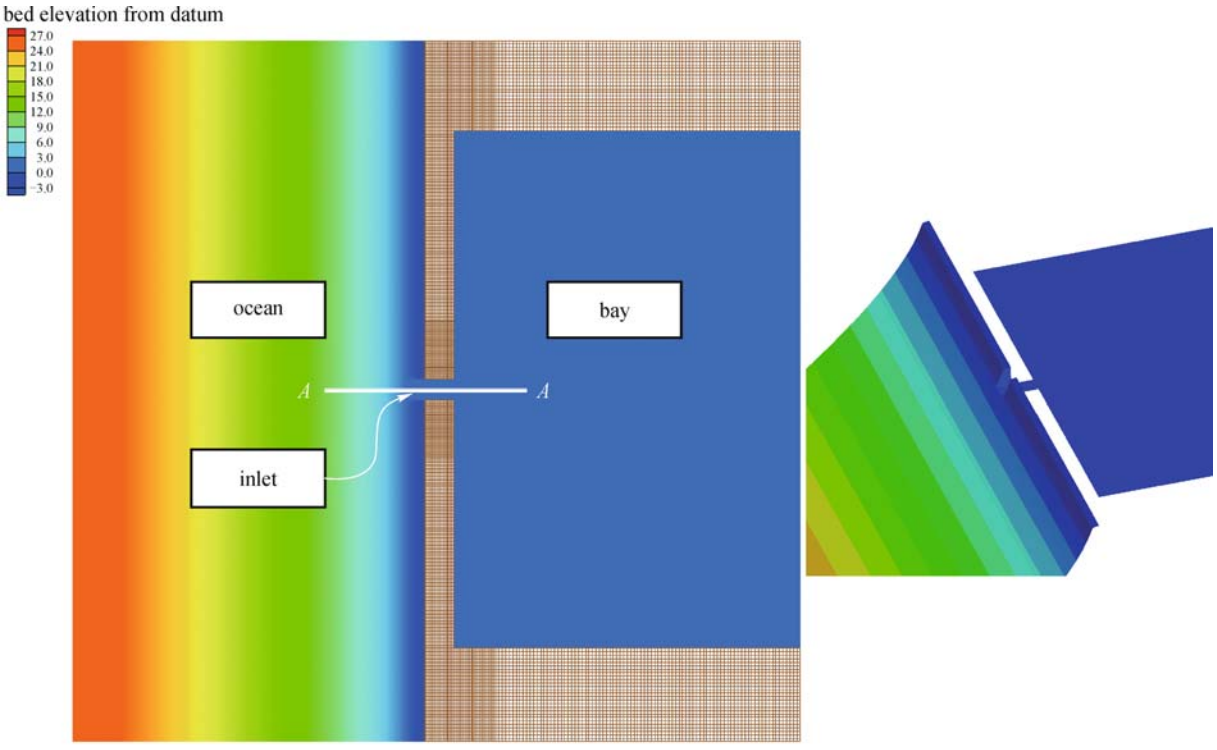


**Fig. 5** Idealized coastal inlet with initial bathymetry

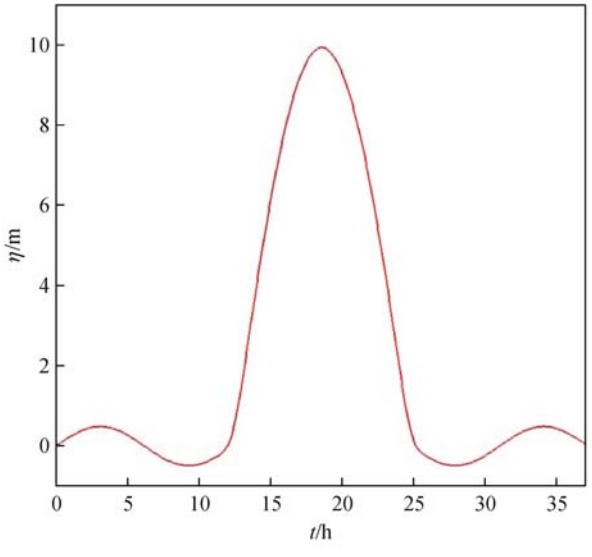


**Fig. 6** Storm surge imposed at offshore boundary

study need further investigations to determine the accuracy of the model, it can be stated that the present model can be applied to study wave-current-morphodynamic processes. The shock capturing property of the hydrodynamic model helps to simulate the complex flow scenario in the inlet when attacked by a severe storm.

### 4.3 Overflow and overwash driven by storm surges and waves in a coast with an inlet

A coast is generally protected by levees or barrier islands and storm surges are allowed to pass through the inlet channel. However, during extreme hydrological conditions, the inlet channel may not be able to divert excessive flow and hence water may overflow the levees or barrier islands. During overflow, the top portion is overwashed by currents induced by storm surges. As a result, levee crests may be eroded by the overwash flow. Such flow condition and the corresponding morphological changes are simulated herein. The flow and wave conditions are kept same as the previous example only the geometry is modified to represent levee in between ocean and bay (Fig. 10). For clarity, the levee is shown separately in the same Fig. 10. To demonstrate an overwash current by the surge tide as shown in Fig. 6, the crest level of the levees adjacent to the inlet was lowered to 2.0 m above the mean sea level, which is higher than the flood tide level (i.e., 0.5 m above the mean sea level). It is assumed that the levees are formed by coastal sands with the same grain size as that on the sea bed (i.e., $d_{50} = 0.2$ mm). The morphological changes take place around the inlet and are presented in Fig. 11. In this simulation, the storm surge and waves are allowed to overflow the levees, erode the levee crest, and deposit the sands to the toe of the levee at the bay side. This pattern is clearly seen at $t = 19$ h in Fig. 11 (a). At $t = 27$ h, a small

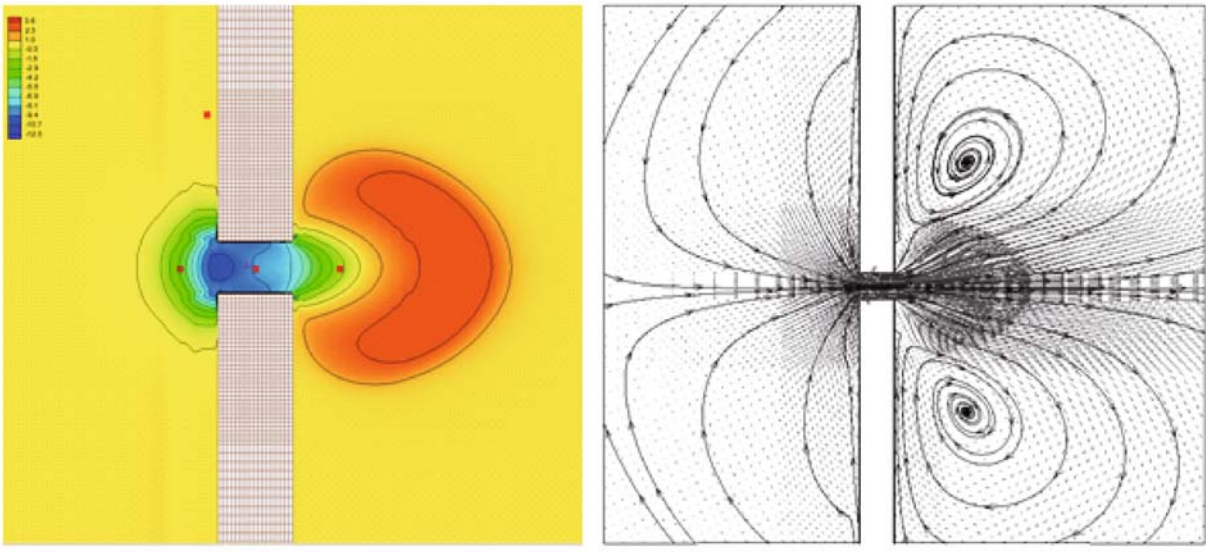

**Fig. 7** Computed results at $t$ = 19 h. (a) Bed elevation change; (b) velocity vectors

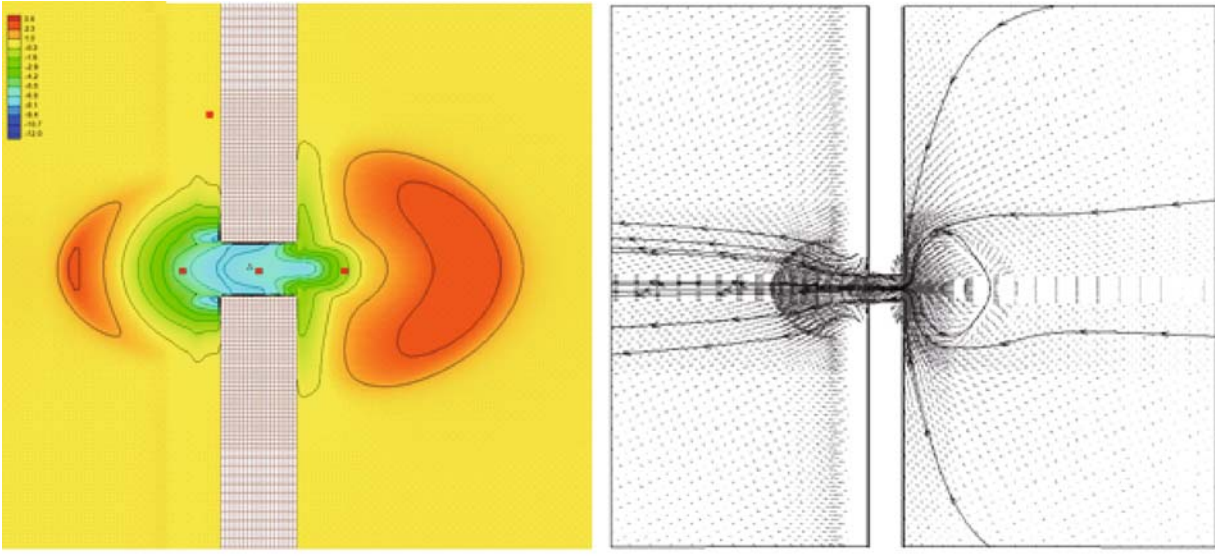

**Fig. 8** Computed results at $t$ = 27 h. (a) Bed elevation change; (b) velocity vectors

portion of the sediments are carried back to the ocean side but the transport rate is not significant (Fig. 11 (b)). Since the overflow and overwash happen over the levees, the flows through the inlet become weaker than the previous case (e.g., Figs. 7 and 8) in which neither overflow nor overwash occurred over the crest of the levees. Therefore, the rate of erosion and deposition in the inlet channel in this condition is not as significant as the previous one. Inside the inlet channel, both sides of the inlet are eroded. After the ebb tide, an ebb shoal appears at the ocean side close to the entrance of the inlet channel (Fig. 11(b)). The computed bed profiles are recorded during the simulation at three transects shown in Fig. 10 and are plotted in Fig. 12 (a)–(c). The bed profiles along the transects *A-A* (along the center line of the inlet), *B-B* (1.6 km north to *A-A*) and *C-C* (1.5 km south to *A-A*) are shown in Fig. 12 (a)–(c). The profiles indicate that due to overflow and overwash erosions on the levee crest and depositions at the toe of the levee are developed. However, inside the inlet channel (Fig. 12 (b)), the bed elevation changes show that a small flood shoal and an ebb shoal are created by the storm surges and waves. The bed morphology pattern predicted by the model is qualitatively representative. However, the model should be validated with real world data.

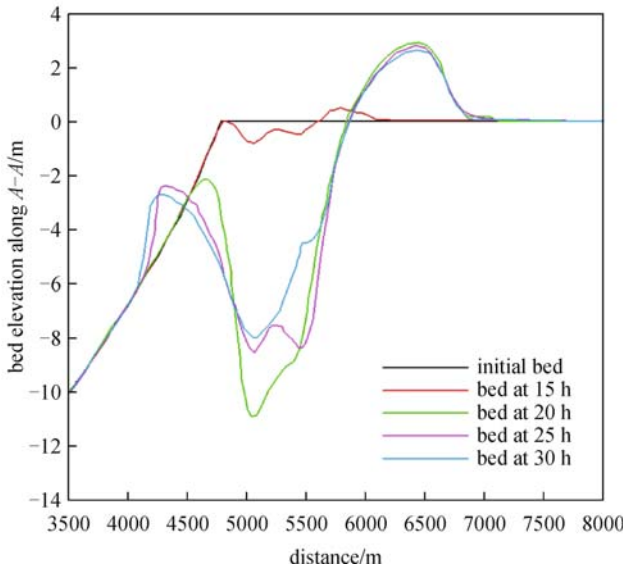


**Fig. 9** Computed bed profile at different times along the transect A-A as shown in Fig. 5

## 5 Conclusions

A numerical model for systematically simulating wave-current-morphodynamic processes in two-dimensions with a focus on modeling supercritical flows such as overflow and overwash driven by storm surges and waves, as well as the corresponding morphological changes is developed. The two-dimensional shallow water equations are solved by a shock-capturing finite volume method considering the effects of wave radiation stress, wind stress, Coriolis force and strong bottom irregularities. The hydrodynamic model is coupled with CMS-Wave [21] and sediment transport models of SMS package [18,22] in order to simulate wave deformation/transformation, currents, and morphological changes in coastal/tidal inlets and their adjacent barrier islands. The accuracy of the presently developed hydrodynamic model is investigated by solving an experimental test case in which a dam-break flow was generated and an overflow over an obstacle in stream was measured. The model results closely follow the experimental observations on the propagations of the supercritical dam-break flow and the overflow over the obstacle. The applicability of the model is tested by simulating a storm surge attacking a medium size idealized coast with an inlet and barrier islands. The successful simulations show that the storm surge causes significant bed erosion, deposition, overflow, overwash and formation of flood and ebb shoals. The overall results seem to be satisfactory and representative for preliminary investigation of applicability of such a process based numerical model and further study is required to examine the predictive accuracy of the model.

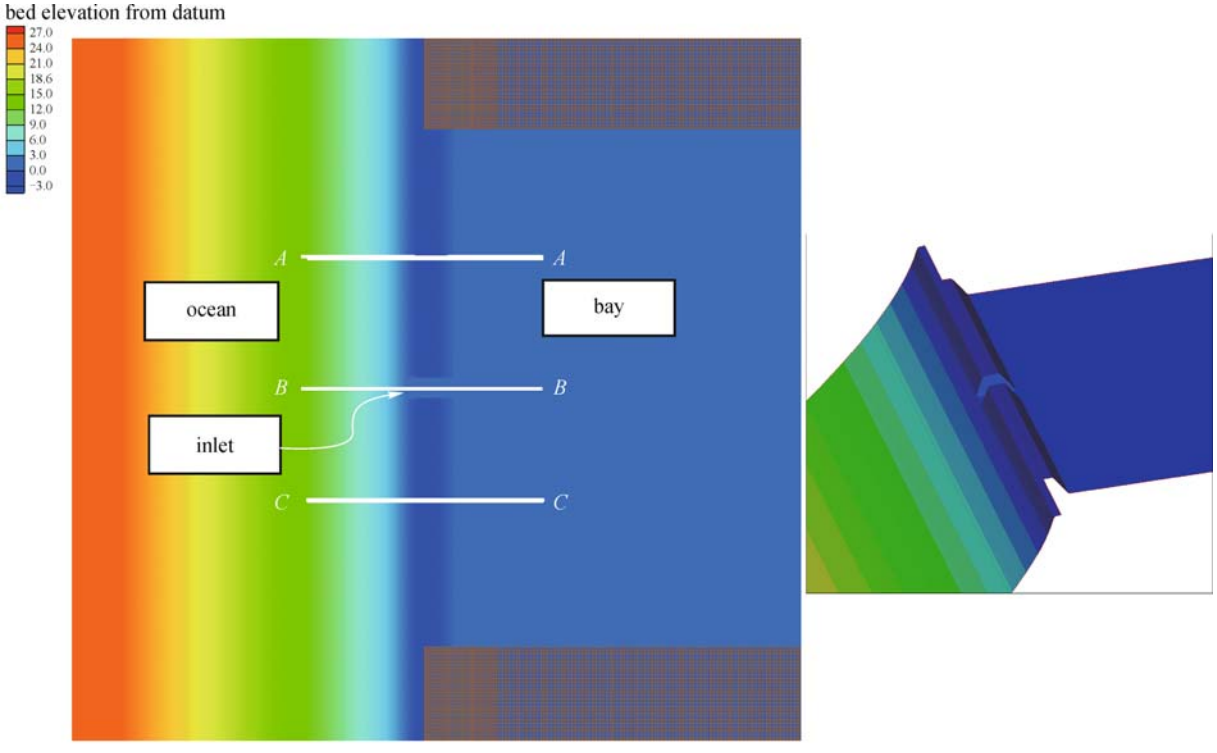


**Fig. 10** Idealized coastal inlet with initial bathymetry and barrier island

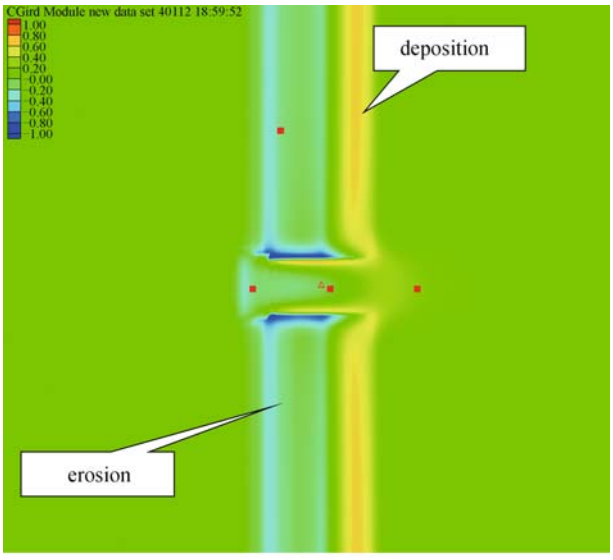


(a)

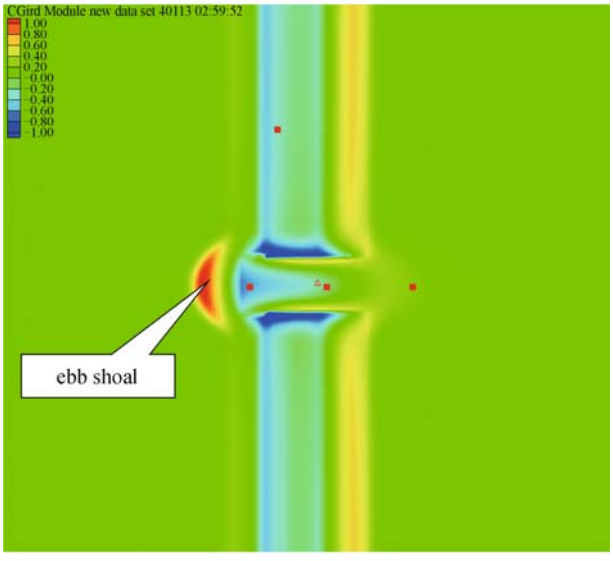


(b)

**Fig. 11** Bed morphological changes at (a) a flood tide at $t$ = 19 h and (b) an ebb tide at $t$ = 27 h

**Acknowledgements** This work was a product of research partially sponsored by USACE-ERDC's Coastal and Hydraulics Laboratory (CHL) under contract No. W912HZ-06-C-0003 and the National Center for Computational Hydroscience and Engineering (NCCHE) at the University of Mississippi, USA. The first author had conducted this study in the NCCHE from 2008 to 2010.

## References

1. Briaud J L, Chen H C, Govindasamy A V, Storesund R. Levee Erosion by Overtopping in New Orleans during the Katrina Hurricane. Journal of Geotechnical and Geoenvironmental Engineering, 2008, 134(5): 618–632
2. Fritz H M, Blount C, Sokoloski R, Singleton J, Fuggle A, McAdoo

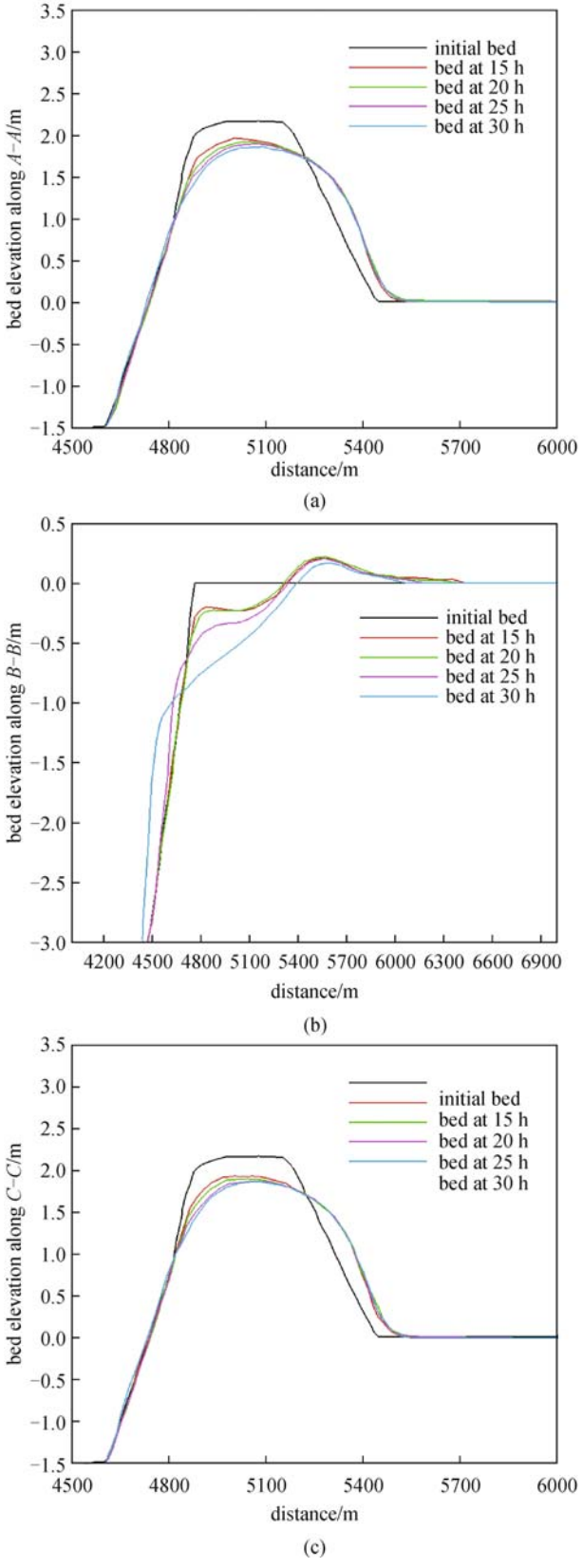


**Fig. 12** Computed bed profiles at different times along the transects. (a) A-A; (b) B-B; (c) C-C as shown in Fig. 10

B G, Moore A, Grass C, Tate B. Hurricane katrina storm surge reconnaissance. Journal of Geotechnical and Geoenvironmental Engineering, 2008, 134(5): 644–656

3. LACPR. Louisiana Coastal Protection and Restoration: Final Technical Report (LACPR). U S Army Corps of Engineers, New Orleans District, Mississippi Valley Division, 2009 (http://lacpr.usace.army.mil/default.aspx?p = LACPR_Final_Technical_Report)
4. Mississippi Coastal Improvements Program (MsCIP). Hancock, Harrison, and Jackson Counties, Mississippi Comprehensive Plan and Integrated Programmatic Environmental Impact Statement, VOLUME 1–MAIN REPORT, US Army Corps of Engineers Mobile District, 2010 (http://www.sam.usace.army.mil/mscip/MsCIP_Comprehensive_Plan.htm)
5. Steetzel H J. Cross-shore transport during storm surges. Dissertation Degreee for the Doctoral Degree. Delft: TU Delft, 1993
6. Overton M F, Fisher J S, Young M A. Laboratory investigation of dune erosion. Journal of Waterway, Port, Coastal, and Ocean Engineering, 1988, 114(3): 367–373
7. Nishi R, Kraus N C. Mechanism and calculation of sand dune erosion by storms. In: Proceedings of the 25th Coastal Engineering Conference. ASCE, 1996, 3034–3047
8. Stockdon H F, Holman R A, Howd P A, Sallenger A H. Empirical parameterization of setup, swash, and runup. Coastal Engineering, 53, 573–588 University Delft. ISBN 90–9006345–5, CASPARIE publishers, Zwolle, 2006
9. Schäuffer H A. Edge waves forced by short-wave groups. Journal of Fluid Mechanics, 1994, 259(-1): 125–148
10. Erikson L, Larson M,Hanson H. Prediction of swash motion and Run-up. 2005
11. Roelvink J A. Surf beat and its effect on cross-shore profiles. Dissertation for the Doctoral Degree. Delft: Delft University of Technology, 1993
12. van Dongeren A, Reniers A, Battjes J, Svendsen I. Numerical modeling of infragravity wave response during DELILAH. Journal of Geophysical Research: Oceans (1978–2012), 2003, 108(C9): 1–19
13. Reniers A J H M, Roelvink J A, Thornton E B. Morphodynamic modelling of an embayed beach under wave group forcing. Journal of Geophysical Research, 2004, 109(C1): C01030
14. Roelvink, J A, van Kessel, T, Alfageme S, Canizares R. Modelling of barrier island response to storms. In: Proceedings Coastal Sediments'03. Clearwater, Florida (CD Rom). 2003
15. Militello A, Kraus N C. Numerical simulation of sediment pathways at an idealized inlet and ebb shoals. In: Proceeding of Coastal Sediments 03. CD-ROM published by World Scientific Publishing (ISBN 981–238–422–7), 2003
16. Ding Y, Wang S S Y. Development of a numerical model for simulating morphodynamic processes driven by tides and waves at coastal inlets. In: Proceeding of the Tenth International Conference on Estuarine and Coastal Modeling Congress 2007. Malcolm L. Spaulding, Editors Newport, Rhode Island, USA, November 5–7, 2007, 862–878
17. Lesser G R, Roelvink J A, van Kester J A T M, Stelling G S. Development and validation of a three-dimensional morphological model. Coastal Engineering, 2004, 51(8–9): 883–915
18. Buttolph A M, Reed C W, Kraus N C, Ono N, Larson M, Camenen B, Hanson H, Wamsley T, Zundel A K. Two-dimensional depth-averaged circulation model CMS-M2D: Verson 3.0, Report 2, sediment transport and morphology change. Technical Report ERDC/CHL-TR-06–7.U S. Army Engineer Research and Development Center, Vicksburg, M S, USA, 2006
19. Ding Y,Wang,S S Y. Development and application of coastal and estuarine morphological process modeling system. Journal of Coastal Research, 2008, 52: 127–140
20. Kuiry S N, Ding Y, Wang S S Y. Modeling coastal barrier breaching flows with well-balanced shock-capturing technique. Computers & Fluids, 2010, 39(10): 2051–2068
21. Lin L, Demirbilek Z, Mase H, Zheng J H, Yamada F. CMS-wave: A nearshore spectral wave processes model for coastal inlets and navigation projects. Coastal Inlets Research Program, Coastal and Hydraulics Laboratory Technical Report ERDC/CHL-TR-08–13. US Army Engineer Research and Development Center, Vicksburg, MS, USA, 2008
22. Zundel A K. Surface-water Modeling System reference manual. Brigham Young University, Environmental Modeling Research Laboratory, Provo, UT, 2000
23. Harten A, Lax P D, Van Leer B. On upstream differencing and Godunov-type schemes for hyperbolic conservation laws. SIAM Review, 25 (1), 35–61 Including the effects of swash interaction. Coastal Engineering 52, 285–302 infragravity wave response during DELILAH. Journal of Geophysical Research, 1983, 108(C9): 3288
24. Camenen B, Larson M. A bed load sediment transport formula for the nearshore. Estuarine, Coastal and Shelf Science, 2005, 63(1–2): 249–260
25. Ding Y, Wang S S Y. Implementation of an efficient and accurate implicit solution scheme for the IMS-M2D hydrodynamic model. National Center for Computational Hydroscience and Engineering, University of Mississippi, Interim Contract Report for U S. Army Engineer research and Development Center, Coastal and Hydraulics Laboratory, February, 2006
26. Leonard B P. A stable and accurate convective modelling procedure based on quadratic upstreaminterpolation. Computer Methods in Applied Mechanics and Engineering, 1979, 19(1): 59–98
27. Mase H. Multidirectional random wave transformation model based on energy balance equation. Coastal Engineering, 2001, 43(04): 317–337
28. Mase H, Amamori H, Takayama T. Wave prediction model in wave-current coexisting field. In: Proceedings 12th Canadian Coastal Conference (CD-ROM). 2005
29. Brufau P, García-Navarro P A, Vázquez-Cendón M E. Zero mass errorusing unsteady wetting-drying conditions in shallow flows over dry irregular topography. International Journal for Numerical Methods in Fluids, 2004, 45(10): 1047–1082